



Letter

Enhanced mechanical property of Fe–Al alloy due to Mn insertion: *ab initio* study



Seung Jin Kang^a, Sora Park^b, Miyoung Kim^a, Heung Nam Han^a, Suk-Kyu Lee^c, Kyoo Young Lee^c, Young-Kyun Kwon^{b,*}

^a Department of Materials Science and Engineering, Seoul National University, Seoul 151-742, Republic of Korea

^b Department of Physics and Research Institute for Basic Sciences, Kyung Hee University, Seoul 130-701, Republic of Korea

^c Automotive Steel Products Research Group, Technical Research Laboratories, POSCO, Kwangyang 545-090, Republic of Korea

ARTICLE INFO

Article history:

Received 9 July 2013

Received in revised form 23 August 2013

Accepted 26 August 2013

Available online 5 September 2013

Keywords:

Iron alloy

Mechanical property

Density functional theory

Disordered structure

ABSTRACT

We use *ab initio* density functional theory to examine the structural and mechanical properties of Fe–Al alloys at various Al concentrations with or without a small amount of Mn. For each disordered Fe–Al alloy, we consider sundry disordered configurations to determine the equilibrium structure. It is found that the disordered Fe–Al alloy with high Al content (~25 at%) becomes less stable and more brittle than its ordered counterpart $D0_3$ second phase. To predict the ductility of Fe–Al alloys, we estimate Pugh's constant defined by the ratio between bulk and shear moduli and apply the Pugh's criterion. We find that an addition of a small amount of Mn may stabilize disordered solid solutions over the $D0_3$ second phase. Moreover, the Mn addition also improves its mechanical properties making the disordered Fe–Al alloy more ductile than $D0_3$.

© 2013 Elsevier B.V. All rights reserved.

In recent years, there are increasing demands for novel advanced high strength steels (AHSS) with high ductility, which are essential for fuel-efficient and safer vehicles. High alloying steels containing light element Al have been considered as promising candidates for materials with the high strength–ductility balance and light weight. However, extremely brittle property at high Al content impedes Fe–Al alloys for the industrial applications [1]. There are two primary factors closely related to the brittleness of Fe–Al alloys. Second phase formation is known to be responsible for the brittleness of Fe–Al alloy in high Al concentration range [2]. Surface reaction of Fe–Al alloys with the environmentally delivered hydrogen [3] is another important factor. While many researchers have reported various approaches to avoid the hydrogen effect [4–6], mechanical properties in individual phases have rarely been studied because of difficulties in separating the structure effect from others. Theoretical studies have been performed to understand the interplay between the mechanical properties and the geometrical structures; previous literatures reported the formation energies and the electronic/magnetic properties of ordered alloy structures with 25 at% and 50 at% of Al concentration [7–10]. The mechanical and electronic properties of disordered structures were reported as well [11].

Although a variety of theoretical studies have been performed, those computational results or predictions, unfortunately, are not always consistent with experimental results. Such discrepancy could be ascribed to a rather small unit cell size (16 atoms or so in a unit cell), which is too small to describe the disordered structures. Moreover, theoretical studies did not cover a broad range of Al atom concentration x in $Fe_{1-x}Al_x$, but were restricted only at a few values of concentration [11]. Here, we report mechanical properties of Fe-based alloys in disordered solid solutions (α -Fe) obtained using first-principles density functional theory (DFT) with large unit cell sizes in a broad range of added atom concentration. Our theoretical calculations have focused on examining ductility on the basis of the order–disordered second phase transition and study the possibility for light steel with desirable mechanical properties. Our calculated data in the whole concentration range reveal the trends of their mechanical and physical properties. Additionally, we present the role of Mn addition in disordered Fe–Al alloy, motivated by twinning induced plasticity (TWIP) steel containing 15–25 wt% of Mn concentration with 2 wt% Al and 4 wt% Si additions, which exhibits high strength and exceptional ductility [12]. In contrast to the TWIP steel, our study focuses on the influence of a small amount of Mn in the Fe alloy with high Al content. We found that a small amount of Mn enhances structural stability and ductility of disordered Fe–Al alloy and evades forming an ordered second phase.

To explore the physical properties of various Fe-based alloys, we used first-principles DFT [13] based on the norm-conserving

* Corresponding author. Tel.: +82 2 961 9279

E-mail address: ykkwon@khu.ac.kr (Y.-K. Kwon).

Table 1

Calculated lattice constant a in Å, formation energy ΔE_f in eV, and magnetic moments per atom, μ , in μ_B , Bohr magneton of known iron–aluminum alloy structures. The D0₃ structure contains 25 at% of Al concentration, while B2 and B32 structures are at 50 at%. The bcc iron structure is selected as a reference for the formation energy comparison. Data in brackets are experimental data for Fe [37], theoretical formation energy for D0₃, B2 and B32 [8] and magnetic momentum data for D0₃, B2 [7].

	a (Å)	ΔE_f (eV/atom)	μ (μ_B)
Fe (bcc)	2.86 (2.87)	0.00 (0.00)	2.27
D0 ₃ : Fe ₃ Al	5.81 (5.77)	−0.34 (−0.33)	1.71 (2.06)
B2: FeAl	2.87 (2.89)	−0.53 (−0.62)	0.5 (0.75)
B32: FeAl	5.90 (5.90)	−0.33 (−0.31)	1.63

pseudopotential method [14] with separable non-local operators [15]. Atomic orbitals basis (SIESTA package) with double- ζ polarization was used to expand the electron wave functions with an energy cutoff of 200 Ry for the real-space mesh [16]. For exchange-correlation (XC) functional, the generalized gradient approximation (GGA) [17] with spin polarization was used. We sample the small Brillouin zone with 8 k -points in order to represent the Bloch wave functions for the momentum-space integration. To confirm the reliance of the data, we also performed DFT calculations based on projector augmented wave (PAW) method [18,19] with VASP package [20–23]. The wave functions were expanded with plane wave basis with 400 eV of energy cutoff and Perdew and Wang XC functional is used [24,25].

The reliability of our computational technique was verified by testing our technique with bulk bcc Fe, D0₃, B2 and B32 structures. First, we performed a series of geometry relaxation calculations to find the equilibrium structure. Our calculated formation energy ΔE_f in eV, lattice constant a in Å and magnetic moments μ in μ_B (Bohr magneton) are compared to those obtained in previous studies [7,8]. As summarized in Table 1, our results agree well with previous results, indicating that our technique can be applied to describe Fe–Al alloy structures and explain their thermodynamic phase diagram.

To investigate the physical properties of structures with Fe_{1-x}Al_x ($0 < x < 0.5$) and their formation energies, it is required to find the equilibrium geometry with disordered configuration for a given Al atom concentration. A “perfect” disordered alloy structure could only be formed with an infinite system. In practice, however, we can examine only super cells with a finite size of a quasi-disordered structure. A larger super cell improves its disorderedness at the cost of significantly increased computational time. Here, we chose a

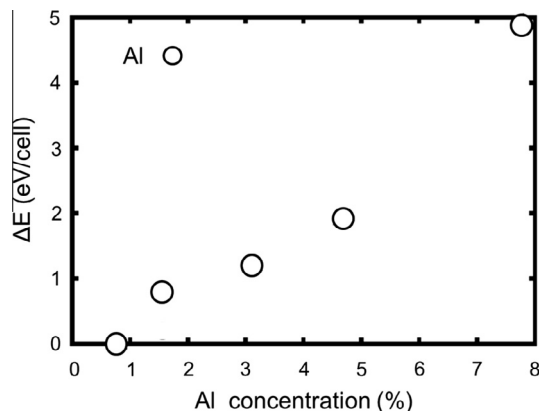


Fig. 2. Total energy difference defined by ($\Delta E = E_{\text{agg}} - E_{\text{dis}}$, where E_{agg} and E_{dis} are the total energy of the aggregated and dispersed configurations of Fe_{1-x}Al_x systems as a function of Al atom concentration. Positive ΔE means that the dispersed Al atom configuration is more stable than the aggregated one with the same Al concentration.

128-atom unit up to 10 at% of added atom concentrations ($x \approx 0.78, 1.56, 3.12, 4.68, 7.81, 8.59, 9.38$ at%) to compromise between disorderedness and computation time. Over 10 at% of concentration ($x \approx 12.96, 20.37, 22.22, 27.77, 29.62, 38.89, 55.55$ at%), we used a 54-atom unit cell to reduce the computational time. For structural relaxation, all the atoms in the unit cell were fully relaxed by conjugate-gradient method [26] until none of the residual Hellmann-Feynman forces acting on any atom exceeded 0.001 Ry/ a_B , where a_B is the Bohr radius. The Murnaghan equation of state was used to fit the total energy as a function of volume.

First, various distributions of added Al atoms in disordered structures were examined to find the most stable configuration of Fe_{1-x}Al_x for a given concentration of x . We considered two extreme configurations. In one configuration, the added atoms were aggregated to form a cluster by themselves within a unit cell, while in the other configuration, they were dispersed not to form any direct bonds with other added atoms. The total energy differences between these two cases, defined by $\Delta E = E_{\text{agg}} - E_{\text{dis}}$, where E_{agg} (E_{dis}) is the total energy of the aggregated (dispersed) configuration, were calculated as a function of their concentration. The calculated ΔE values are all positive suggesting that the dispersed configurations are energetically preferred for Fe–Al alloy as displayed on Fig. 2. Therefore we chose the disordered structures

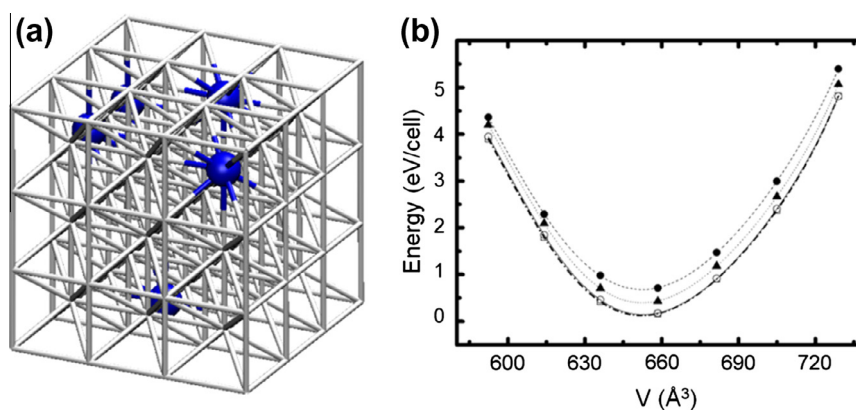


Fig. 1. (a) A typical configuration of disordered Fe_{1-x}Al_x at $x \approx 0.039$ containing 5 Al atoms denoted by dark (blue) spheres and 123 Fe atoms represented by lattice points connected by bonds. Note that 37 Fe atoms are missing for better display of the bcc lattice structure. Many more configurations were similarly generated by distributing Al atoms in a disordered manner. (b) Total energy curves as a function of cell volume V in Å³ for selected disordered configurations among many different disordered configurations with the same x . The configuration represented with thick solid line, which is the most stable structure, was selected as an equilibrium disordered structure for a given concentration x . (For interpretation of the references to color in this figure legend, the reader is referred to the web version of this article.)

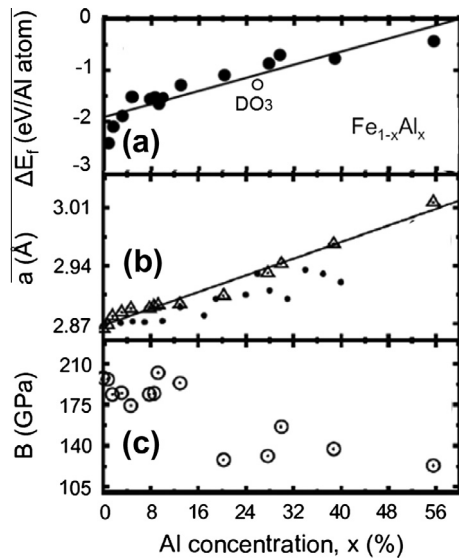


Fig. 3. (a) Formation energy ΔE_f , (b) lattice constant and (c) bulk modulus B of disordered $\text{Fe}_{1-x}\text{Al}_x$ as a function of Al concentrations. Result for Fe–Al alloys are displayed in columns. For the ΔE_f the value of DO_3 phase is displayed with a hollow circle for the comparison with the disordered phase. Experimental lattice constant data for Al [28] is represented with circle dots on (b).

where Al atoms are distributed without direct bonding between Al atoms within a super cell. This enabled us to reduce the total number of configurations to be considered to determine the equilibrium disordered structure for a given concentration of added atoms. We studied considerable numbers of configurations for the dispersed cases (at least 3 cases for each Al concentration), although not all the configurations, which could be adopted as disordered structures. Total energy curves for dispersive configurations are shown in Fig. 1(b). We found that the total energy differences among those calculated configurations are typically less than 4 meV per atom as long as added atoms are not clustered. We chose stable configuration for subsequent calculations for physical and mechanical properties.

The corresponding physical properties of disordered solid solutions, discussed in Fig. 1(a) and (b), are calculated. The formation energy of $\text{Fe}_{1-x}\text{Al}_x$ with Al atom concentration x was calculated from the total energy of the bulk Fe (bcc) and the bulk Al (fcc) structures. The formation energy of Fe–Al solid solutions decreases with Al concentrations as shown in Fig. 3(a) which shows reasonable agreement with the experimental values, especially at low Al concentrations [27]. As listed in Table 1, DO_3 and B2 crystal structures of Fe–Al alloy, which have 25 at% and 50 at% of Al concentrations, are more stable than the corresponding solid solutions. This is consistent with the known phase diagram for Fe–Al binary alloy. The B32 structure of 50 at% of Al concentration is less stable than B2, DO_3 structure, as predicted in an earlier study with full

potential LAPW method [8]. Lattice constant increases with increasing Al concentration (Fig. 3(b)). At low Al concentrations, the agreement is reasonable with the experimental values [28], but the discrepancy increases with increasing Al concentration. This discrepancy could be ascribed to the second phase (DO_3 , B2) formation in the experimental condition. Fig. 3(c) shows bulk modulus of Fe–Al. Significant reduction in bulk modulus with increasing Al concentration presents the same trend as previous *ab initio* calculations [9,29]. Comparing the bulk moduli of solid solution structures shown in Fig. 3(c) with those of second phases listed in Table 2, we found that the B2 structure appears to have higher bulk modulus than its disordered counterpart with a similar concentration, whereas the bulk modulus of DO_3 structure is essentially similar to that of disordered ones.

We further explored the mechanical properties of Fe–Al alloy in terms of Al concentration by calculating various elastic moduli and investigating ductility. To evaluate ductility, we used the Pugh's criterion which states that a material is ductile (brittle) if $\nu > 1.75$ ($\nu < 1.75$), where ν is Pugh's constant defined by the ratio of bulk modulus B to shear modulus G , i.e. $\nu = B/G$. It is known that the Pugh's criterion [30] can be used for materials whose melting temperatures are above $T_p \approx 1198$ K for pure elements. It has been reported that small shear modulus could cause multiple shear bands, which elongate largely without fracture. If extensive elongation acts dominantly on the material, the fracture would appear easily [31]. Recently, the Pugh's criterion was applied to disordered Fe–Mg, Fe–Cr to estimate their ductility and reasonably verified the experimental values [32]. The ductility of alloys of rare earth elements and transition metals was also successfully predicted with this criterion [33]. Since the melting points of Fe–Al alloys [34] are well above T_p [9], the Pugh's criterion may also work to describe the ductility of Fe–Al alloy.

To estimate the shear moduli of disordered solid structures, we applied monoclinic and tetragonal strains with no volume change and performed geometrical relaxation while keeping the deformation. Elastic constants were obtained by fitting the changes in energy under these strains for selected configurations of $\text{Fe}_{1-x}\text{Al}_x$ with $x = 13/54$ and $4/54$. For the comparison, we also represent the energy changes for the DO_3 , B2 second phase corresponding to $x = 0.25$, $x = 0.5$ respectively. For the shear modulus G , we used uniform strain condition of Voigt [34], $G = (C_{11} - C_{12} + 3C_{44})/5$. This condition could well describe elastic properties of single crystalline materials. The calculated ν values are given in Table 2, where we summarized other elastic data obtained using both methods with atomic orbitals basis and with plane wave basis. Pugh's constant of DO_3 and B2 structures are below 1.75, successfully reproducing experimentally observed brittleness of the Fe–Al alloys with high Al content. At low concentration of Al (e.g., at $x \approx 0.074$ or 7.4 at%), disordered Fe–Al alloy almost keeps the Pugh's constant presenting ductile property. But around 25 at% of Al concentration (≈ 24.1 at%), the Pugh's constant falls a way below the Pugh's criterion value $\nu = 1.75$, suggesting brittle characteristics in disordered phase, even worse than DO_3 and B2 structures as shown in

Table 2

Calculated elastic constants C_{11} – C_{22} , C_{44} , B , G and $\nu = B/G$ of various solid solutions: $\text{Fe}_{1-x}\text{Al}_x$ ($\text{Fe}_{54-x}\text{Al}_x$) and $\text{Fe}_{1-x-y}\text{Al}_x\text{Mn}_y$ ($\text{Fe}_{54-x-y}\text{Al}_x\text{Mn}_y$) for $x = 4/54$ ($X = 4$), $x = 13/54$ ($X = 13$), and $x = 13/54$ ($X = 13$) with $y = 3/54$ ($Y = 3$), and DO_3 and B2 crystal structures corresponding to $x = 0.25$ and $x = 0.5$, as well as pure Fe bcc crystal structure. Values in brackets for the high Al concentrations were calculated using plane wave basis, and those in square brackets for Fe are experimental data obtained at $T = 4.2$ K by Rayne and Chandrasekhar [38].

Composition	C_{11} – C_{12}	C_{44}	B	G	ν
Fe	87.4 [105]	101 [121.9]	181 [173.1]	77.8 [87.5]	2.33 [1.98]
$\text{Fe}_{50}\text{Al}_4$	57.8	117.6	190	82.1	2.31
$\text{Fe}_{41}\text{Al}_{13}$	33 (55)	156.4 (141)	154.3 (146)	100.5 (95.6)	1.54 (1.54)
$\text{Fe}_{38}\text{Al}_{13}\text{Mn}_3$	27 (56)	120 (128)	143 (157)	77 (88)	1.86 (1.78)
DO_3 (Fe_3Al)	38.6	134	152	88	1.72
B2 (FeAl)	131	143	176	112	1.57

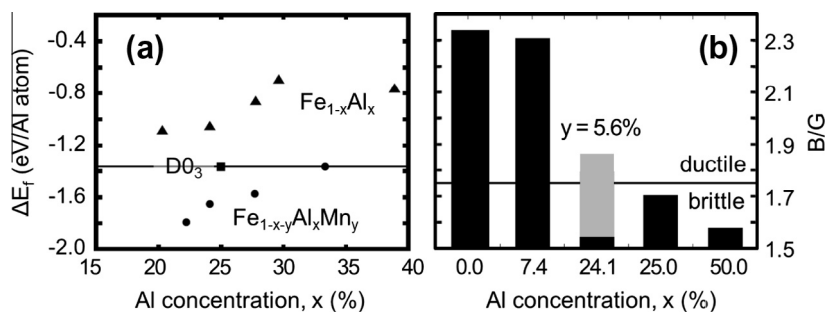


Fig. 4. (a) Formation energy of $\text{Fe}_{1-x}\text{Al}_x$ and $\text{Fe}_{1-x-y}\text{Al}_x\text{Mn}_y$ disordered structures as a function of Al concentration x , depicted by solid triangles and solid circles, respectively. The Mn content is fixed at $y \approx 5.6$ at%. The formation energy of the D0_3 structure is depicted by solid square with a solid line, below (above) which the structures are more (less) stable than the D0_3 structure. Mn addition stabilizes the Fe–Al disordered structure even more than D0_3 structure. (b) Bar graph of the calculated Pugh's constants of various structures. Substitution of Mn in high Fe–Al disordered structure increases the Pugh's constant implying ductile property. The bars at 25 at% and 50 at% of Al concentration correspond to D0_3 and B2 structures.

Fig. 4(b) and Table 2. This interesting and unexpected finding implies that even if a disordered solid solution phase could persist near 25 at% of Al concentration, its ductility would be significantly deteriorated.

In search of the possibility for having ductile and light alloy, we noticed a report that Mn atoms could influence the ductile property of the alloys by modifying the magnetic property which prefers certain slip systems [35]. To investigate the role of Mn addition in disordered Fe–Al alloy, we randomly substituted Mn atoms into Fe atoms in a disordered manner while keeping Al concentration, which is the same method as used to model the disordered Fe–Al alloy. The most energetically favorable disordered configuration was chosen after taking into accounts 3 different cases. For the formation energy calculations, the concentration of Mn is fixed to ≈ 5.6 at%, while Al concentration is varied over 20–40 at% range (Fig. 4(a)). To estimate Pugh's constant by calculating the elastic constants, only a single case of ≈ 24.1 at% Al with ≈ 5.6 at% Mn was considered (Fig. 4(b)). We found that second phase formation could be suppressed by Mn content in Fe–Al alloy steel by changing the energetic preference of second phases. Fig. 4(a) displays the calculated formation energy of $\text{Fe}_{1-x-y}\text{Al}_x\text{Mn}_y$ disordered structure as a function of Al content compared to that of $\text{Fe}_{1-x}\text{Al}_x$ disordered solid solution. As a reference, a solid horizontal line passing through the formation energy of the D0_3 structure is displayed. For a given Al concentration, the structure with the formation energy below the line is more stable than that with higher formation energy. It is clear that near 25 at% of Al content, a 5.6 at% addition of Mn improves the stability of disordered Fe–Al alloy, which becomes even more stable than D0_3 structure. This matches the TEM observation results which showed lowered amount of ordered D0_3 structure in Fe–28Al–1.5Mn [36]. Through this result, we propose that a disordered structure would be formed easily at high Al concentration, if small amount of Mn is included in the solid solution. More importantly, its ductile property was enhanced in the presence of Mn atoms. Fig. 4(b) summarizes the calculated Pugh's constants of selected disordered structures as well as of D0_3 and B2 ordered configurations. Though disordered Fe–Al (Al ≈ 24.1 at%) has much lower Pugh's constant than 1.75, small amount of Mn (5.6 at%) in disordered phase lifts the Pugh's constant more than $\nu = 1.75$.

In conclusion, we performed first principles density functional theory calculations to understand the fundamental properties of iron-based alloys $\text{Fe}_{1-x}\text{Al}_x$. We found that Al atoms substituted for Fe atoms are distributed in a disordered fashion without self-clustering. It was shown that Fe–Al alloys exhibit unusual structural and elastic properties. Especially for Fe–Al alloy, at low concentrations of the Al atoms, disordered solid solution structures are energetically preferred with similar mechanical properties to

those of the pure bulk iron system. In contrast, at high concentrations, especially around 25 at%, ordered second phases, such as D0_3 structure, are found to be more stable than its disordered counterparts with a similar Al content. At high concentration, not only the second phase structures, but also disordered configurations exhibit degraded mechanical and elastic properties. We found that the formation of second phases may be suppressed by incorporation of Mn atoms. Furthermore, we found that Mn atom addition improves the ductility of the alloy, which shows the paths to achieve ductile and light Fe alloys.

Acknowledgments

YKK and SP have been supported by National Research Foundation of Korea (NRF-2009-0074951 and NRF-2011-0016188). SJK and MK acknowledge support by Basic Science Research Program through the National Research Foundation of Korea (NRF) funded by the Ministry of Education, Science and Technology (No. 20110002504). HNH was supported by the Converging Research Center Program (2011K000599) through the Ministry of Education, Science and Technology of Korea government. Some portion of our computational work was done using the resources of the KISTI Supercomputing Center (KSC-2012-C2-72 and KSC-2013-C2-024).

References

- [1] N. Stoloff, *Materials Science and Engineering A* 258 (1998) 1.
- [2] M. Marcinkowski, M. Taylor, F. Kayser, *Journal of Materials Science* 10 (1975) 406.
- [3] D. Kasul, L. Heldt, *Metallurgical and Materials Transactions A* 25 (1994) 1285.
- [4] R. Baligidad, U. Prakash, A. Radhakrishna, *Materials Science and Engineering A* 255 (1998) 162.
- [5] Y. Huang, W. Yang, G. Chen, Z. Sun, *Intermetallics* 9 (2001) 331.
- [6] S. Yangshan, Y. Zhengjun, Z. Zhonghua, H. Haibo, *Scripta Metallurgica et Materialia* 33 (1995) 811.
- [7] G. Das, B. Rao, P. Jena, S. Deevi, *Physical Review B* 66 (2002) 184203.
- [8] P.G. Gonzales-Ormeño, H.M. Petrilli, C.G. Schön, *Calphad* 26 (2002) 573.
- [9] P.G. Gonzales-Ormeño, H.M. Petrilli, C.G. Schön, *Scripta Materialia* 54 (2006) 1271.
- [10] F. Lechermann, F. Welsch, C. Elsässer, C. Ederer, M. Fähnle, J.M. Sanchez, B. Meyer, *Physical Review B* 65 (2002) 132104.
- [11] F. Plazaola, J. Garitaonandia, *The European Physical Journal B-Condensed Matter and Complex Systems* 31 (2003) 167.
- [12] O. Grässel, L. Krüger, G. Frommeyer, L. Meyer, *International Journal of Plasticity* 16 (2000) 1391.
- [13] P. Hohenberg, L.J. Sham, *Physical Review A* 140 (1965) 1133.
- [14] N. Troullier, J.L. Martins, *Physical Review B* 43 (1991) 1993.
- [15] L. Kleinman, D. Bylander, *Physical Review Letters* 48 (1982) 1425.
- [16] J.M. Soler, E. Artacho, J.D. Gale, A. García, J. Junquera, P. Ordejón, D. Sánchez-Portal, *Journal of Physics: Condensed Matter* 14 (2002) 2745.
- [17] J.P. Perdew, K. Burke, M. Ernzerhof, *Physical Review Letters* 77 (1996) 3865.
- [18] P.E. Blöchl, *Physical Review B* 50 (1994) 17953.
- [19] G. Kresse, D. Joubert, *Physical Review B* 59 (1999) 1758.
- [20] G. Kresse, J. Furthmüller, *Physical Review B* 54 (1996) 11169.

- [21] G. Kresse, J. Furthmüller, *Computational Materials Science* 6 (1996) 15.
- [22] G. Kresse, J. Hafner, *Physical Review B* 47 (1993) 558.
- [23] G. Kresse, J. Hafner, *Physical Review B* 49 (1994) 14251.
- [24] J.P. Perdew, J.A. Chevary, S.H. Vosko, K.A. Jackson, M.R. Pederson, D.J. Singh, C. Fiolhais, *Physical Review B* 46 (1992) 6671.
- [25] J.P. Perdew, J.A. Chevary, S.H. Vosko, K.A. Jackson, M.R. Pederson, D.J. Singh, C. Fiolhais, *Physical Review B* 48 (1993) 4978.
- [26] M.R. Hestenes, E. Stiefel, NBS, 1952.
- [27] S. Radcliffe, B. Averbach, M. Cohen, *Acta Metallurgica* 9 (1961) 169.
- [28] H. Sheng, Y. Zhao, Z. Hu, K. Lu, *Physical Review B* 56 (1997) 2302.
- [29] H. Zhang, M.P. Punkkinen, B. Johansson, S. Hertzman, L. Vitos, *Physical Review B* 81 (2010) 184105.
- [30] S. Pugh, *Philosophical Magazine* 45 (1954) 823.
- [31] J. Schroers, W.L. Johnson, *Physical Review Letters* 93 (2004) 255506.
- [32] H. Zhang, B. Johansson, L. Vitos, *Physical Review B* 79 (2009) 224201.
- [33] J.R. Morris, Y. Ye, Y.-B. Lee, B.N. Harmon, K.A. Gschneidner Jr, A.M. Russell, *Acta Materialia* 52 (2004) 4849.
- [34] W. Voigt, Leipzig, Teubner, 962 (1928).
- [35] P. Lazar, R. Podlousky, *Intermetallics* 17 (2009) 675.
- [36] B. Lou, X. Zhang, M. Liu, Z. Mao, *Journal of Materials Science* 34 (1999) 1025.
- [37] C. Kittel, P. McEuen, *Introduction to Solid State Physics*, vol. 7, Wiley, New York, 1996.
- [38] J. Rayne, B. Chandrasekhar, *Physical Review* 122 (1961) 1714.